Bioresource Technology 101 (2010) 3153–3158

Contents lists available at ScienceDirect

Bioresource Technology

journal homepage: www.elsevier.com/locate/biortech

Artificial neural network-genetic algorithm based optimization for the immobilization of cellulase on the smart polymer Eudragit L-100

Yu Zhang [a,b], Jingliang Xu [a], Zhenhong Yuan [a,*], Huijuan Xu [a], Qiang Yu [a,b]

[a] Key Laboratory of Renewable Energy and Gas Hydrate, Guangzhou Institute of Energy Conversion, Chinese Academy of Sciences, Guangzhou 510640, PR China
[b] Graduate University of Chinese Academy of Sciences, Beijing 100049, PR China

ARTICLE INFO

Article history:
Received 5 October 2009
Received in revised form 18 December 2009
Accepted 19 December 2009
Available online 12 January 2010

Keywords:
Immobilized cellulase
Artificial neural network
Smart biocatalysis
Response surface methodology
Genetic algorithm

ABSTRACT

Cellulase was covalently immobilized on a smart polymer, Eudragit L-100 by carbodiimide coupling. Using data of central composite design, response surface methodology (RSM) and artificial neural network (ANN) were developed to investigate the effect of pH, carbodiimide concentration, and coupling time on the activity yield of immobilized cellulase. Results showed simulation and prediction accuracy of ANN was apparently higher compared to RSM. The maximum activity yield obtained from RSM was 57.56% at pH 5.54, carbodiimide concentration 0.32%, and coupling time 3.03 h, where the experimental value was 60.87 ± 4.79%. Using ANN as fitness function, a maximum activity yield of 69.83% was searched by genetic algorithm at pH 5.07, carbodiimide concentration 0.36%, and coupling time 4.10 h, where the experimental value was 66.75 ± 5.21%. ANN gave a 9.7% increase of activity yield over RSM. After reusing immobilized cellulase for 5 cycles, the remaining productivity was over 50%.

1. Introduction

Cellulase has large potential value in many industries, such as bioenergy, food, animal feed, textile, paper and pulping (Bhat, 2000; Himmel et al., 1999; Li et al., 2009; Percival Zhang et al., 2006). However, its application has been restricted because of expensive production (Himmel et al., 1999). In order to improve the economy of cellulase utilization, the immobilization technology has been studied extensively (Filos et al., 2006; Li et al., 2007; Liao et al., 2008; Wu et al., 2005). Cellulase that has been immobilized on soluble carriers is capable of hydrolyzing insoluble cellulosic substrates, but recovery of the enzyme is still difficult and stability has not been improved evidently via the modification. When immobilized on insoluble carriers, limited hydrolysis of cellulosic substrates by such immobilized cellulase is inevitable as a result of poor contact (Woodward, 1989). Use of smart or stimuli-responsive polymers as carriers has been suggested as a good solution to these problems (Galaev and Mattiasson, 2002; Roy et al., 2004). As one of the smart polymers, Eudragit L-100 (a copolymer of metacetic acidrylic acid and methyl metacetic acidrylate) has always been used to immobilize enzymes by covalent (Cong et al., 1995; Smith et al., 2008; Taniguchi et al., 1989) or non-covalent methods (Gaur et al., 2005; Rajoka et al., 2007; Roy et al., 2003; Sardar et al., 2000).

Because Eudragit L-100 could not adsorb cellulase strongly and the adsorption may be affected negatively by the presence of xylanase (Roy and Gupta, 2006; Sardar et al., 2000), covalent coupling of cellulase to the polymer is required to obtain excellent performance of immobilized cellulase. In our preliminary research, the covalent immobilization (carbodiimide coupling) provided a Eudragit-cellulase bioconjugate with good operational stability but low activity yield (less than 30%) at pH 5.0, EDC 0.6%, and time 6 h as described by others (Dourado et al., 2002; Taniguchi et al., 1989). It may be caused by either excess or lacking coupling between enzyme and Eudragit. Excess coupling could affect the structure of cellulase active center, and lacking coupling could decrease the loading of cellulase on Eudragit. Therefore, the coupling protocol needed to be optimized to improve the activity yield of immobilized cellulase.

The conventional one-factor-at-a-time approach of optimization process is not only laborious but also ignores the combined interaction of each factor. In contrast, artificial neural network (ANN) could identify arbitrary discriminant functions directly from experimental data (Almeida, 2002). Moreover, it is a superior and more accurate modelling technique than response surface methodology (RSM) as ANN represents the non-linearity in a much better way (Desai et al., 2008; Singh et al., 2008; Tompos et al., 2007). As the most popular artificial learning tool in biotechnology, ANN has been applied in constructing models of many complicated bioprocesses such as functional analysis of genomic/proteomic sequences, microbial metabolism, and enzymatic reaction (Almeida, 2002; Pal et al., 2009; Szaleniec et al., 2006; Tompos et al., 2007;

* Corresponding author. Tel.: +86 20 87057735; fax: +86 20 87057737.
E-mail address: yuanzh@ms.giec.ac.cn (Z. Yuan).

0960-8524/$ - see front matter © 2009 Elsevier Ltd. All rights reserved.
doi:10.1016/j.biortech.2009.12.080

Wang and Wan, 2009; Zhang et al., 2009). The modelled ANN could be considered as the fitness function for optimization by genetic algorithm (GA). GA uses evolutionary natural selection processes, where selection results in species that fit the best. Recently, ANN (combined with GA) has gradually become a more and more popular approach to solve optimization problems in many bioprocesses without theoretical or mechanistic dependence (Serra et al., 2003; Singh et al., 2008; Wang and Wan, 2009).

In the present investigation, a novel coupling conditions optimization technique based on ANN (as compared with RSM usually used) was developed to improve the activity yield of immobilized cellulase.

2. Methods

2.1. Materials

Eudragit L-100 was obtained from Degussa Ltd. (Shenzhen, China). The polymer is completely soluble above pH 4.3 in water solution, and the critical soluble pH changed to 5.0 via coupling cellulase (Taniguchi et al., 1989).

1-Ethyl-3-(3-dimethyllaminopropyl) carbodiimide (EDC) that was used as coupling agent, was purchased from Sigma–Aldrich (Shanghai, China). Filter paper was provided by Whatman Ltd. (Guangzhou, China). Crude cellulase powder (74.07 FPU/g) was provided by Shanghai Bio Life Science and Technology Co., Ltd. of China. FPU is the activity unit of cellulase when filter paper is used as substrate. All other reagents were of the highest purity available.

2.2. Enzyme assay

Cellulase activity (FPU) was measured by the Commission on Biotechnology of the International Union of Pure and Applied Chemistry (IUPAC) (Ghose, 1987). For the assay procedures described here, 2.0 mg of reducing sugars (glucose equivalents) were produced from filter paper (1×6 cm, about 50 mg) at some diluted enzyme solution.

2.3. Immobilization of cellulase on Eudragit L-100

One gram of Eudragit L-100 was dissolved in a 40 ml of distilled water in a flask and then pH of the solution was brought to 11 with drop wise addition of 3 M NaOH. After the polymer dissolved completely, the pH value of the solution was decreased to 4.32–7.68 by adding 1 mol/l HCl and the total volume was made up to 50 ml with distilled water. To the polymer solution, carbodiimide (0.06–0.74%, w/v) was added to activate the polymer for 15 min, and then crude cellulase powder containing 100 mg protein was added and kept under stirring for 0.48–5.52 h at room temperature. After the desired time, the pH value of the mixture was reduced to 3.6 with 3 mol/l acetic acid. Precipitations were separated by centrifugation (10,000rpm, 10 min) at 4.0 °C. In order to remove the adsorbed cellulase, the obtained precipitations were washed three times with 0.02 mol/l acetic acid (containing 1 mol/l NaCl and $CaCl_2$) and used as immobilized cellulase. Dissolve immobilized cellulase with 0.2 mol/l acetate buffer (pH 5.0) to some diluted solution and assay its activity as the description of Section 2.2. Activity yield, which was taken as the response of the designed experiments, was calculated as follow:

$$\text{activity yield } (\%) = \frac{\text{activity of immobilized cellulase}}{\text{activity of free cellulase}} \times 100 \quad (1)$$

Table 1
Experimental range and levels of each factor.

Factors	Symbol	Range and levels				
		−1.68	−1.00	0.00	1.00	1.68
pH	X_1	4.32	5.00	6.00	7.00	7.68
EDC concentration (%)	X_2	0.08	0.16	0.28	0.40	0.48
Coupling time (h)	X_3	0.48	1.5	3.0	4.5	5.52

2.4. Central composite design

Activity yield is determined by the coupling between Eudragit and cellulase. Besides carbodiimide concentration (coupling agent) and coupling time, pH that is important for stability and life of carbodiimide in water solution, could also affect the coupling reaction. The range and levels of the three factors investigated in this study were given in Table 1, and were also chosen to encompass the range in the literature (Silva et al., 2006; Smith et al., 2008). A composite design (CCD) with 20 trials was generated by Minitab statistical software. The central composite design consisted of a 2^3 full factorial design at a distance 1.68179 from the origin and 6 central points (Table 2). Using RSM and ANN models, the combined effect of the three factors was evaluated according to the experimental results of the CCD.

2.5. Response surface methodology

The relationship amongst the three factors was expressed in a second-order equation:

$$Y = a_0 + \sum_{i=1}^{3} a_i X_i + \sum_{i=1}^{3} \sum_{j=1}^{3} a_{ij} X_i X_j \quad (2)$$

where, Y is the predicted activity yield, a_0 is constant, a_i and a_{ij} are the regression coefficients of RSM model, X_i and X_j is the factor variable. Statistical analysis of the data from CCD was performed to evaluate the analysis of variance (ANOVA) using Minitab statistical software.

2.6. Artificial neural network

In our experiment, the ANN architecture consists of three neurons (pH, carbodiimide concentration, and coupling time) in the in-

Table 2
CCD matrix of three factors and the experimental, RSM and ANN determined values of activity yield. Trails 1 to 14 and 15 to 20 are the experimental runs at the axial and center points, respectively.

Trial	X_1	X_2	X_3	Activity yield (%)		
				Experimental	RSM	ANN
1	−1.00	−1.00	−1.00	54.35 ± 3.09	45.53	54.36
2	+1.00	−1.00	−1.00	39.71 ± 2.71	40.23	38.99
3	−1.00	+1.00	−1.00	40.97 ± 3.73	36.87	39.25
4	+1.00	+1.00	−1.00	39.29 ± 2.38	34.79	38.28
5	−1.00	−1.00	+1.00	52.81 ± 3.06	50.94	52.95
6	+1.00	−1.00	+1.00	34.99 ± 2.14	32.72	34.94
7	−1.00	+1.00	+1.00	43.54 ± 3.23	36.65	42.8
8	+1.00	+1.00	+1.00	19.20 ± 1.08	21.65	19.94
9	−1.68	0.00	0.00	37.44 ± 2.97	47.28	38.59
10	+1.68	0.00	0.00	31.04 ± 2.65	30.23	30.84
11	0.00	−1.68	0.00	40.44 ± 4.03	44.67	40.88
12	0.00	+1.68	0.00	23.33 ± 1.84	27.91	24.2
13	0.00	0.00	−1.68	36.23 ± 3.19	43.22	39.65
14	0.00	0.00	+1.68	34.69 ± 2.71	36.73	34.59
15	0.00	0.00	0.00	55.65 ± 4.74	55.42	55.75
16	0.00	0.00	0.00	55.65 ± 4.74	55.42	55.75
17	0.00	0.00	0.00	55.65 ± 4.74	55.42	55.75
18	0.00	0.00	0.00	55.65 ± 4.74	55.42	55.75
19	0.00	0.00	0.00	55.65 ± 4.74	55.42	55.75
20	0.00	0.00	0.00	55.65 ± 4.74	55.42	55.75

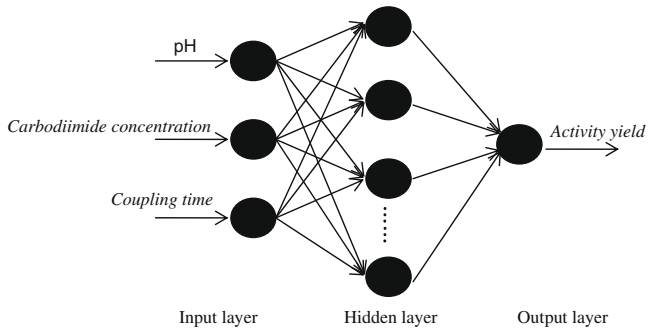

Fig. 1. Schematic representation of ANN modelling the relationship between activity yield and three factors (pH, carbodiimide concentration, and coupling time).

put layer, four neurons in the hidden layer, and one neuron (activity yield) in the output layer (Fig. 1). All the data (input and output ones) were scaled as follow:

$$X^* = 2\frac{X - X_{\min}}{X_{\max} - X_{\min}} - 1$$
$$Y^* = \frac{Y - 0}{100 - 0} \quad (3)$$

where, X^* and Y^* are the new scaled data of input and output layers. The new scaled data were fed to train an ANN model using back-propagation algorithm. The tangent sigmoid and pure linear functions were used as the transfer functions in the hidden and output layers of the ANN, respectively. The mean square error between the results of the output neurons and the actual outputs is calculated and propagated backward through the network. Then the algorithm adjusts the weight of each. Once the mean square error got to 1e−4, the training was over and the corresponding ANN was built.

2.7. Enzymatic hydrolysis insoluble celluloses by immobilized cellulase

To check the reusability of immobilized cellulase, repeated hydrolysis reaction was carried out. 5 FPU of immobilized cellulase was incubated with 0.5 g microcrystal cellulose at 50 °C and pH 5.0 with constant shaking at 120 rpm. The total reaction volume was 25 ml. After 60 min, undegraded substrate was separated by centrifugation at 10,000 rpm for 5 min. For recovering enzyme, the pH of the obtained supernatant was reduced to 3.6 with 2 M acetic acid, followed by centrifugation at 8000 rpm for 10 min. The recovered precipitation (immobilized cellulase) was washed three times with 0.02 M acetic acid and used for the next hydrolytic reaction at the same conditions. After recovering immobilized cellulase, DNS method was used to estimate the amount of reducing sugars produced (Ghose, 1987).

Rice straw was also hydrolyzed as describe above but pretreated in advance. 10 g rice straw was boiled with 300 ml NaOH solution (w/v, 2%) for 60 min at normal pressure.

3. Results and discussion

3.1. Response surface methodology

RSM is a frequently used technique for building models and determining the optimal process conditions. Based on the experimental results of CCD in Table 2, a quadratic polynomial was established to identify the relationship between activity yield and three immobilization conditions. The resulting RSM model equation is following:

$$Y = -196.069 + 70.6313X_1 + 97.6285X_2 + 28.1013X_3 - 5.90640X_1^2 - 165.447X_2^2 - 2.43215X_3^2 + 4.02500X_1X_2 - 2.15333X_1X_3 - 4.69167X_2X_3 \quad (4)$$

where, Y = response value (activity yield), X_1 = pH, X_2 = carbodiimide concentration, X_3 = coupling time.

According t and p-values shown in Table 3, the significance of the three factors could be considered as: coupling time > carbodiimide concentration > pH. The larger the t-value and the smaller the p-value is, the higher is the significance of corresponding coefficient. Based on Eq. (4), the 3D response surface diagrams are presented in Fig. 2. From the 3D diagrams, it is easy and convenient to understand the interactions between two factors and activity yield and also locate their optimum levels. The obtained surfaces were convex and symmetric suggesting that there were well defined optimum operating conditions. However, the convexity was so low that the maximum activity yield of immobilized cellulase may not be predicted accurately enough because flat surfaces mean that activity yield may not vary a lot when three factors vary near the optimum points. Fig. 2 also reveals that pH do not show more significant effect on activity yield of immobilized cellulase compared to carbodiimide concentration and coupling time. The predicted maximum of activity yield by the RSM was 57.56%, where X_1 = 5.54, X_2 = 0.32%, X_2 = 3.03 h. Under the optimized conditions, the activity yield obtained experimentally was 60.87 ± 4.79%, which was in accordance with the predicted RSM model.

3.2. Artificial neural network

Using the experimental results in Table 2, ANN was also applied to model the relationship between activity yield and three immobilization conditions. The weight and threshold values of each layer, which determined the structure of the trained ANN, were as follow:

$$net.iw\{1\} = \begin{pmatrix} 0.8901 & 2.1935 & 2.0877 \\ -1.7721 & 2.1255 & -1.6178 \\ -0.2896 & 2.4506 & -2.4003 \\ 3.7043 & 0.8348 & -0.5728 \end{pmatrix}$$

$$net.lw\{2\} = (-0.1899\ 0.2146\ -0.1930\ 0.3537)$$

$$net.b\{1\} = (-2.3781\ 1.2227\ -0.0382\ 4.3496)^T$$

$$net.b\{2\} = (-0.1705)^T$$

3.3. Comparison of RSM and ANN

After RSM and ANN models were built, the experimentally determined and calculated activity yields with the two models

Table 3
Model coefficients by multiple nonlinear regressions.

Model term	Standard error	t-Value	p-Value
Intercept	2.471	22.428	0.000
X_1	1.640	−3.094	0.011
X_2	1.632	−3.022	0.013
X_3	1.640	−1.178	0.266
X_1^2	1.599	−3.693	0.004
X_2^2	1.568	−4.219	0.002
X_3^2	1.599	−3.422	0.007
X_1X_2	2.142	0.376	0.715
X_1X_3	2.142	−1.508	0.162
X_2X_3	2.142	−0.657	0.526

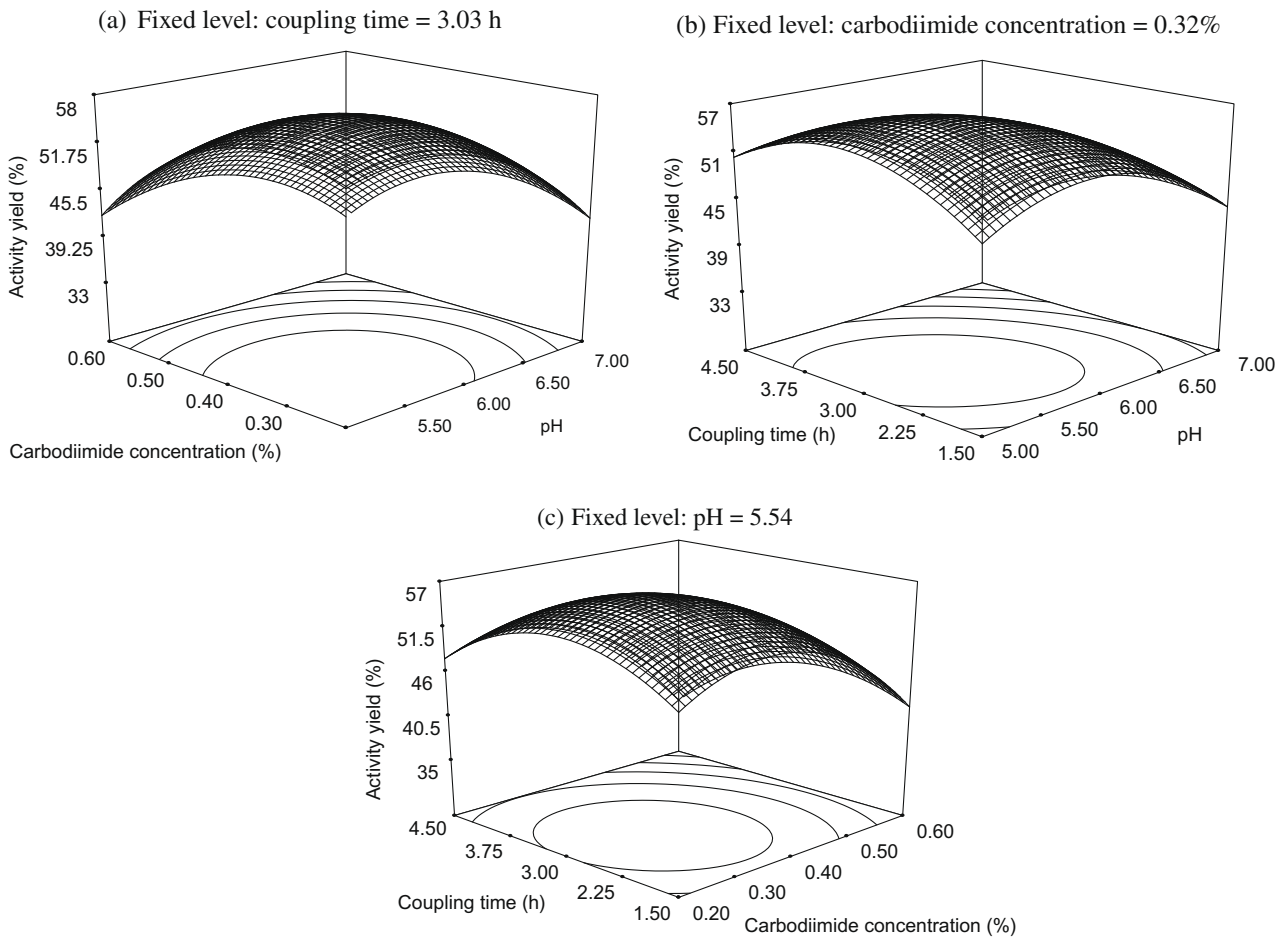

Fig. 2. Three-dimensional response surfaces of activity yield showing the interactions among pH, carbodiimide concentration, and coupling time.

were compared. As seen in Table 2, the experimentally determined and ANN simulated values were almost identical as compared to the simulated values by RSM model. Besides simulation, another three experiments were carried out to examine the predictive performance of the two models (Table 4). Data in Table 4 showed the predicted values by ANN model were much closer to experimentally measured ones. Both simulation and prediction results showed the training of an ANN model was quite successful. The ANN was much more appropriately to be considered as the universal algebraic function between activity yield and the three factors. Similar results were obtained for researchers to study other bioprocesses including enzyme production and enzymatic reaction (Manohar and Divakar, 2005; Singh et al., 2008; Zhang et al., 2009).

3.4. Genetic algorithm

Using the trained ANN as the fitness function, GA was implemented to optimize the immobilization conditions for maximum activity yield as follows. Randomly generate a population of individuals and assign a fitness value to each individual by specific fitness function. Select individuals with higher fitness values and make them undergo genetic operation such as crossover and mutation. Use the newly generated child population as the parent population for the next generation and treat them with the same evolutional process continuously until a stop criterion has been satisfied (He et al., 2008; Izadifar and Jahromi, 2007).

Fig. 3 shows the evolution of the algorithm with successive generations. Starting from 37.91%, the average activity yield apparently increased until about the 30th generation and was 68.41% at the end of 100 generations. The maximum activity yield also had increased quickly for the first 18 generations and got to 69.83% at the 56th generation, then kept invariance. So the maximum activity yield obtained from ANN could be considered as 69.83% that was apparently higher than 57.56% maximized by RSM. The optimum immobilization conditions based on ANN were pH 5.07, carbodiimide concentration 0.36%, and coupling time 4.10 h, where the experimental activity yield was 66.75 ± 5.21%. This showed a perfect agreement with ANN. Compared to the maximum value based on optimum conditions of RSM, there was a 9.7% increase of activity yield.

Table 4
Comparison of experimentally determined, RSM and ANN predicted values of activity yield.

No.	X_1	X_2	X_3	Activity yield (%)		
				Experimental	RSM	ANN
1	−1.68	0.00	1.00	50.37 ± 4.31	45.26	48.43
2	−1.00	1.00	0.00	37.78 ± 2.81	42.19	39.21
3	0.00	1.68	1.68	18.25 ± 2.01	5.13	20.07

3.5. Reusability of immobilized cellulase

Fig. 4 shows the practical application of immobilized cellulase in hydrolysis of insoluble cellulosic substrates. As can be observed, the retained productivity was above 50% after 5 cycles for hydroly-

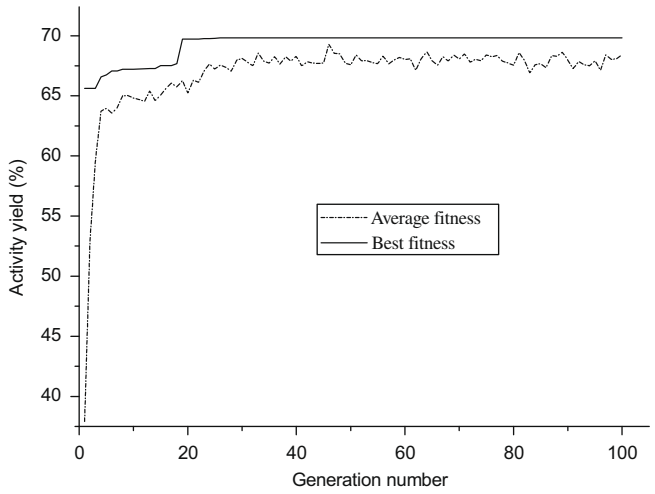

Fig. 3. Evolution of the best and average fitness (activity yield) over the 100 generations in the genetic algorithm.

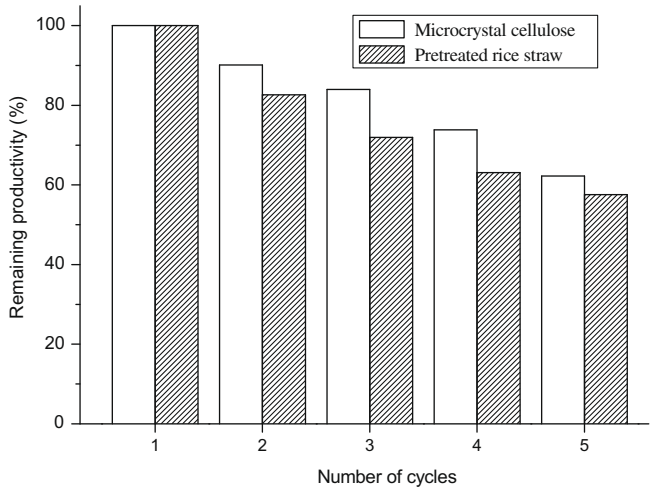

Fig. 4. Reusability of immobilized cellulase for hydrolysis of two insoluble celluloses.

sis of the two insoluble celluloses. It points out that the immobilized cellulase could be mostly recovered during these cycles. The prepared Eudragit-cellulase showed high performance for repeated hydrolysis of insoluble celluloses. Factors causing the loss of the reducing sugars include, but not limited to fall of enzyme from Eudragit due to some weak linkage existence, unavoidable enzyme deactivation during separation and reaction process, and enzyme loss due to adsorption between enzyme and separated substrate.

4. Conclusions

Like the standard RSM, the outputs of ANN can be varied with different data inputs, so ANN also can be employed for modelling and optimization of different bioprocess systems. In this paper, the experimental results showed the simulation and prediction of ANN were superior to that of RSM, and ANN based optimization brought a 9.7% increase of maximum activity yield compared to RSM. It is believed that ANN based optimization technique would gain greater popularity for modelling and optimization of more bioprocess systems due to its mechanistic dependence and high simulation/prediction accuracy shown in learning these systems.

Acknowledgements

This work was funded by the Knowledge Innovation Program of the Chinese Academy of Sciences (KSCX-YW-11-A3, KSCX2-YW-G-075 and KSCX2-YW-G-063), and the National High Technology Research and Development Program of China (863 program, 2007AA05Z406, 2007AA100702-4 and 2009AA05Z436).

References

Almeida, J.S., 2002. Predictive non-linear modeling of complex data by artificial neural networks. Curr. Opin. Biotechnol. 13, 72–76.
Bhat, M.K., 2000. Cellulases and related enzymes in biotechnology. Biotechnol. Adv. 18, 355–383.
Cong, L., Kaul, R., Dissing, U., Mattiasson, B., 1995. A model study on Eudragit and polyethyleneimine as soluble carriers of alpha-amylase for repeated hydrolysis of starch. J. Biotechnol. 42, 75–84.
Desai, K.M., Survase, S.A., Saudagar, P.S., Lele, S.S., Singhal, R.S., 2008. Comparison of artificial neural network (ANN) and response surface methodology (RSM) in fermentation media optimization: case study of fermentative production of scleroglucan. Biochem. Eng. J. 41, 266–273.
Dourado, F., Bastos, M., Mota, M., Gama, F.M., 2002. Studies on the properties of celluclast/Eudragit L-100 conjugate. J. Biotechnol. 99, 121–131.
Filos, G., Tziala, T., Lagios, G., Vynios, D.H., 2006. Preparation of cross-linked cellulases and their application for the enzymatic production of glucose from municipal paper wastes. Prep. Biochem. Biotechnol. 36, 111–125.
Galaev, I., Mattiasson, B., 2002. Smart polymers for bioseparation and bioprocessing, first ed. Taylor and Francis Inc., New York.
Gaur, R., Lata, Khare, S.K., 2005. Immobilization of xylan-degrading enzymes from *Scytalidium thermophilum* on Eudragit L-100. World J. Microbiol. Biotechnol. 21, 1123–1128.
Ghose, T.K., 1987. Measurements of cellulase activities. Pure Appl. Chem. 2, 257–268.
He, L., Xu, Y.Q., Zhang, X.H., 2008. Medium factor optimization and fermentation kinetics for phenazine-1-carboxylic acid production by *Pseudomonas* sp. M18G. Biotechnol. Bioeng. 100, 250–259.
Himmel, M.E., Ruth, M.F., Wyman, C.E., 1999. Cellulase for commodity products from cellulosic biomass. Curr. Opin. Biotechnol. 10, 358–364.
Izadifar, M., Jahromi, M.Z., 2007. Application of genetic algorithm for optimization of vegetable oil hydrogenation process. J. Food Eng. 78, 1–8.
Li, C.Z., Yoshimoto, M., Fukunaga, K., Nakao, K., 2007. Characterization and immobilization of liposome-bound cellulase for hydrolysis of insoluble cellulose. Bioresour. Technol. 98, 1366–1372.
Li, X.H., Yang, H.J., Roy, B., Wang, D., Yue, W.F., Jiang, L.J., Park, E.Y., Miao, Y.G., 2009. The most stirring technology in future: cellulase enzyme and biomass utilization. African J. Biotechnol. 8, 2418–2422.
Liao, H.D., Yuan, L., Tong, C.Y., Zhu, Y.H., Li, D., Liu, X.M., 2008. Immobilization of cellulase based on polyvinyl alcohol/Fe_2O_3 nanoparticles. Chem. J. Chin. Univ. Chin. 29, 1564–1568.
Manohar, B., Divakar, S., 2005. An artificial neural network analysis of porcine pancreas lipase catalysed esterification of anthranilic acid with methanol. Process Biochem. 40, 3372–3376.
Pal, M.P., Vaidya, B.K., Desai, K.M., Joshi, R.M., Nene, S.N., Kulkarni, B.D., 2009. Media optimization for biosurfactant production by *Rhodococcus erythropolis* MTCC 2794: artificial intelligence versus a statistical approach. J. Ind. Microbiol. Biotechnol. 36, 747–756.
Percival Zhang, Y.H., Himmel, M.E., Mielenz, J.R., 2006. Outlook for cellulase improvement: screening and selection strategies. Biotechnol. Adv. 24, 452–481.
Rajoka, M.I., Zia, Y., Khalil-ur-Rehman,, 2007. A surface immobilization method of endoglucanase from *Cellulomonas biazotea* mutant improved catalytic properties of biocatalyst during processing. Protein Pept. Lett. 14, 734–741.
Roy, I., Gupta, M.N., 2006. Design of smart biocatalysts: immobilization of enzymes on smart polymers, second ed. In: Guisan, J.M. (Ed.), Immobilization of Enzymes and Cells. Humana Press Inc., Totowa, pp. 87–95.
Roy, I., Gupta, A., Khare, S.K., Bisaria, V.S., Gupta, M.N., 2003. Immobilization of xylan-degrading enzymes from *Melanocarpus albomyces* IIS 68 on the smart polymer Eudragit L-100. Appl. Microbiol. Biotechnol. 61, 309–313.
Roy, I., Sharma, S., Gupta, M.N., 2004. Smart Biocatalysts: Design and Applications New Trends and Developments in Biochemical Engineering. Springer, Berlin. pp. 159–189.
Sardar, M., Roy, I., Gupta, M.N., 2000. Simultaneous purification and immobilization of *Aspergillus niger* xylanase on the reversibly soluble polymer Eudragit™ L-100. Enzyme Microb. Technol. 27, 672–679.
Serra, J.M., Corma, A., Chica, A., Argente, E., Botti, V., 2003. Can artificial neural networks help the experimentation in catalysis? Catal. Today 81, 393–403.
Silva, C., Gubitz, G., Cavaco-Paulo, A., 2006. Optimisation of a serine protease coupling to Eudragit S-100 by experimental design techniques. J. Chem. Technol. Biotechnol. 81, 8–16.
Singh, A., Majumder, A., Goyal, A., 2008. Artificial intelligence based optimization of exocellular glucansucrase production from *Leuconostoc dextranicum* NRRL B-1146. Bioresour. Technol. 99, 8201–8206.

Smith, E., Zhang, Q., Shen, J., Schroeder, M., Silva, C., 2008. Modification of Esperase® by covalent bonding to Eudragit® polymers L 100 and S 100 for wool fibre surface treatment. Biocatal. Biotransform. 26, 391–398.

Szaleniec, M., Witko, M., Tadeusiewicz, R., Goclon, J., 2006. Application of artificial neural networks and DFT-based parameters for prediction of reaction kinetics of ethylbenzene dehydrogenase. J. Comput. Aided Mol. Des. 20, 145–157.

Taniguchi, M., Kobayashi, M., Fujii, M., 1989. Properties of a reversible soluble insoluble cellulase and its application to repeated hydrolysis of crystalline cellulose. Biotechnol. Bioeng. 34, 1092–1097.

Tompos, A., Margitfalvi, J.L., Tfirst, E., Heberger, K., 2007. Predictive performance of "highly complex" artificial neural networks. Appl. Catal. A: Gen. 324, 90–93.

Wang, J.L., Wan, W., 2009. Application of desirability function based on neural network for optimizing biohydrogen production process. Int. J. Hyd. Energy 34, 1253–1259.

Woodward, J., 1989. Immobilized cellulases for cellulose utilization. J. Biotechnol. 11, 299–312.

Wu, L.L., Yuan, X.Y., Sheng, J., 2005. Immobilization of cellulase in nanofibrous PVA membranes by electrospinning. J. Membr. Sci. 250, 167–173.

Zhang, Y., Xu, J.L., Yuan, Z.H., Zhuang, X.S., Lu, P.M., 2009. Kinetic model study on enzymatic hydrolysis of cellulose using artificial neural networks. Chin. J. Catal. 30, 355–358.